Electronic Supporting Information (ESI)

Functional coatings enable navigation of light-propelled micromotors in blood for effective biodetoxification

Marta Pacheco,[a] Beatriz Jurado-Sánchez*[a,b] and Alberto Escarpa*[a,b]

[a]*Department of Analytical Chemistry, Physical Chemistry and Chemical Engineering, University of Alcalá, Alcalá de Henares, E-28871 Madrid, Spain. E-mail: beatriz.jurado@uah.es; alberto.escarpa@uah.es*

[b]*Chemical Research Institute "Andrés M. del Rio" University of Alcalá, Alcalá de Henares, E-28871 Madrid, Spain.*

Supporting videos

Video S1. Propulsion of PCL/PLGA and PCL micromotors in blood containing 0.22 M of glucose under VIS light irradiation (470 nm).
Video S2. Propulsion of PCL/PLGA micromotors in water containing 0.22 M of glucose without and with a light irradiation (470 nm).

Supporting figures

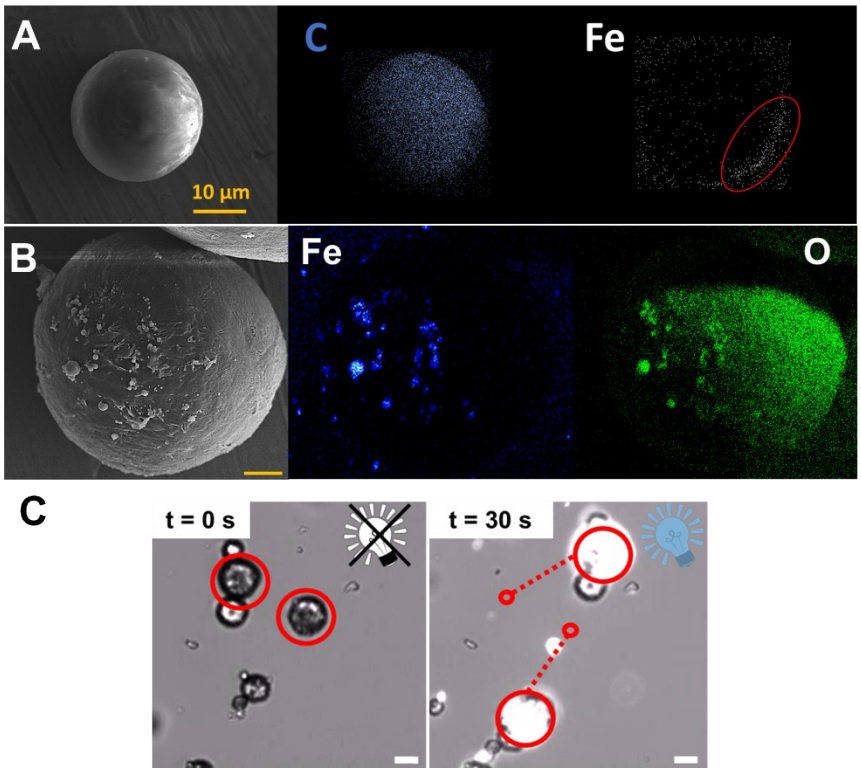

Figure S1. (A, B) SEM and EDX mapping illustrating the morphology and element distribution of two different PCL/PLGA (4:1) micromotor. (C) Time-lapse microscopy images (taken from Video S2) showing the propulsion trajectories of the micromotors in water media over 30 s without (left images) and under (right images) VIS light irradiation (470 nm). Scale bars, 10 µm.

A

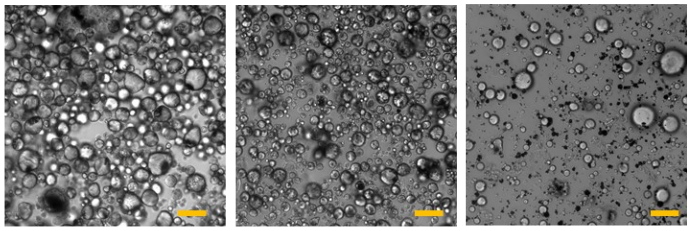

B

	PCL	PCL/PLGA 4:1	PCL/PLGA 1:1
Concentration (micromotors/µL)	37 690 ± 8750	38 330 ± 2800	19000 ± 2450
Size (Ø; µm)	23 ± 12	16 ± 6	14 ± 11

Figure S2. (A) Microscopy images of several micromotors synthesized using different compositions of PCL and PLGA polymers. (B) Table showing the average concentration of micromotors and the size obtained from the different syntheses carried out. Scale bars, 50 µm. The mean size/diameter of the micromotors was obtained by measuring of n = 30.

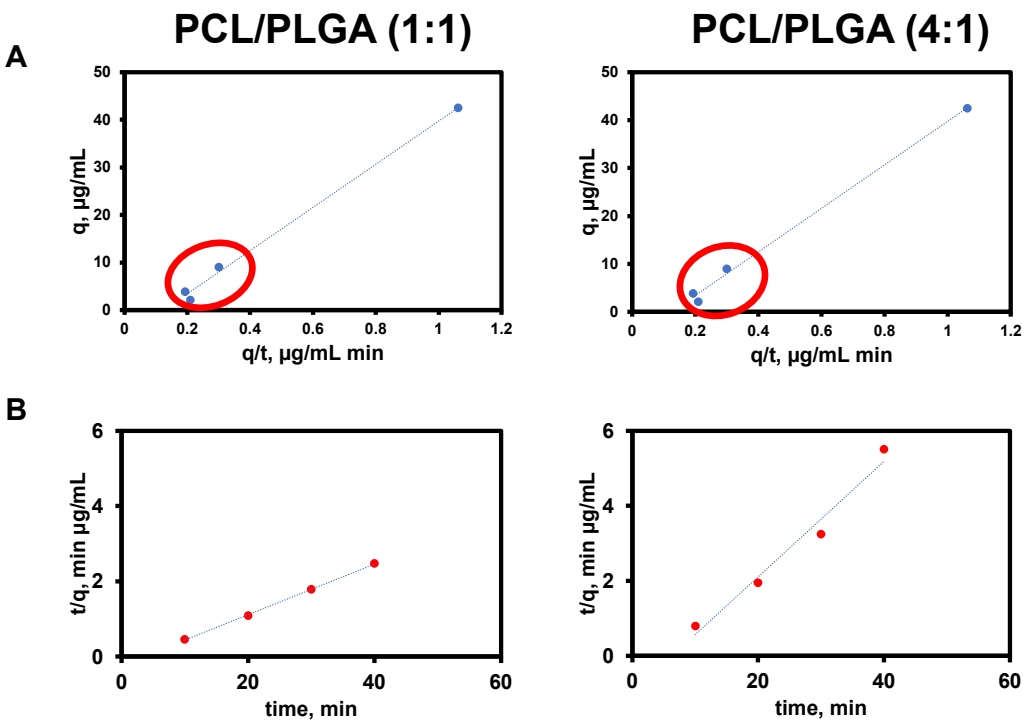

Figure S3. Pseudo second-order kinetic models linearized fits for the sorption of Escherichia coli O111:B4 (A) and α-bungarotoxin (B) using the different micromotors.

A

	ζ-potential (mV) in ultrapure H_2O pH 7.4	*ζ-potential* (mV) in PBS 0.1 M pH 7.4
***Escherichia coli* toxin**	-33.9 ± 0.9	-2.3 ± 1.2
α –bungarotoxin	-17.2 ± 3.6	-3.2 ± 0.8
PCL micromotors	-35.0 ± 4.1	-8.5 ± 0.9
PCL/PLGA 4:1 micromotors	-40.8 ± 0.5	-18.8 ± 0.7

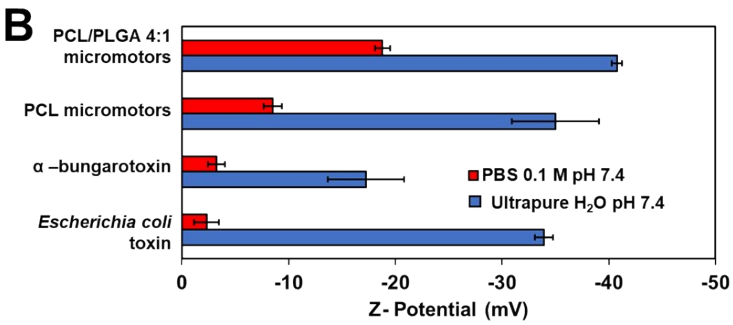

Figure S4. (A) Table and (B) graphic representation of the ζ-potentials of toxins and micromotors in ultrapure water (blue) and PBS 0.1 M PBS (red). The mean of ζ-potentials was obtained by measuring of a number of samples, n = 3.

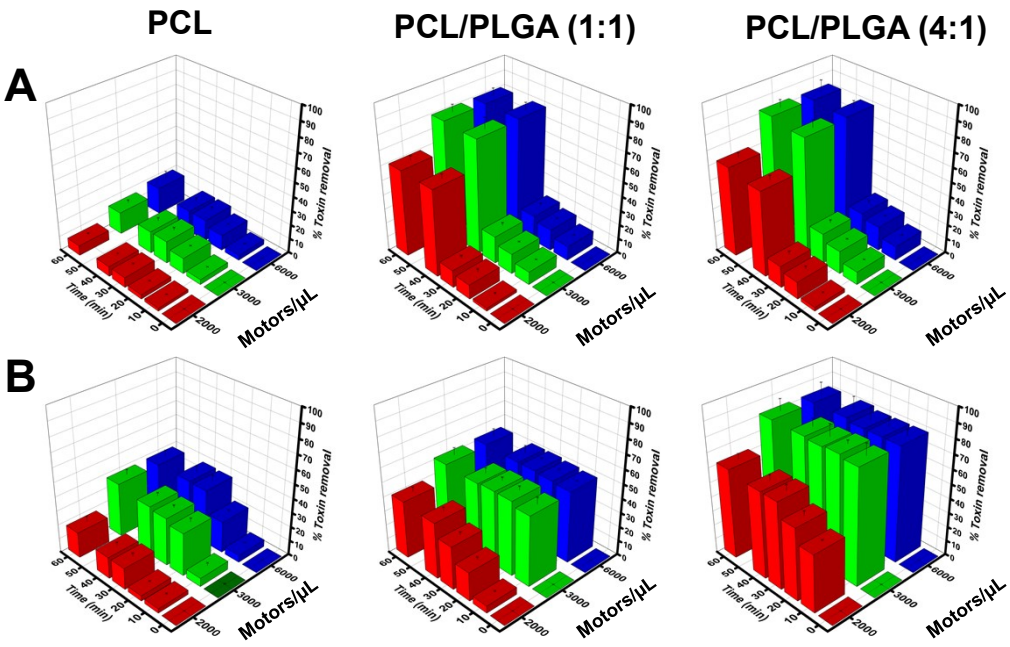

Figure S5. Optimization of the detoxification conditions in blood: effect of time and number of micromotors upon the removal of *Escherichia coli O111:B4* (A) and α-bungarotoxin (B) using PCL, PCL/PLGA (1:1) and PCL/PLGA (4:1) micromotors. Conditions: glucose concentration, 0.22 M, light intensity 470 nm.

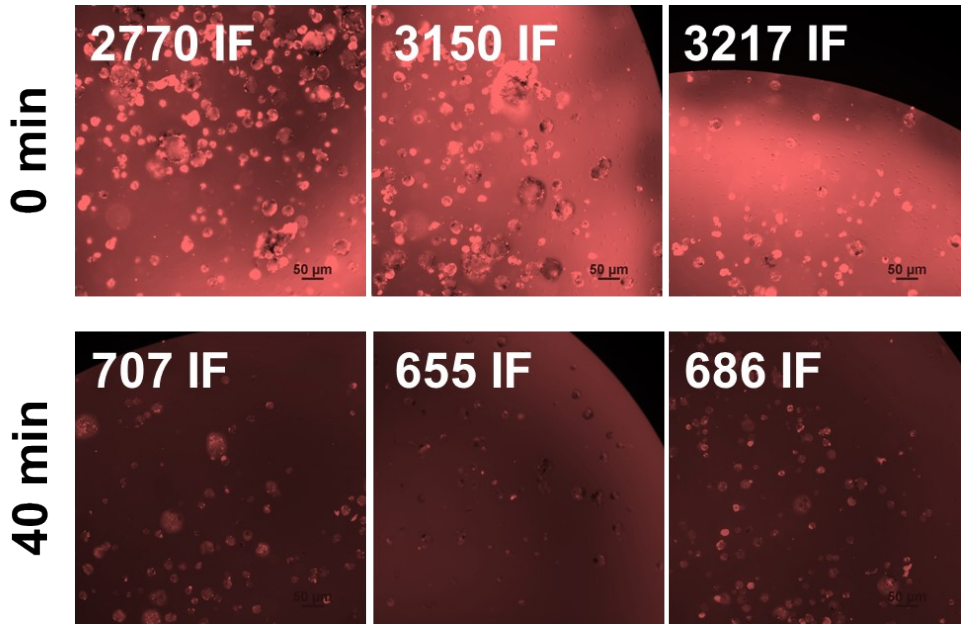

Figure S6. Time-lapse fluorescence images of the native fluorescent decay of the α-bungarotoxin (TMRho labeled) removal by PCL/PLGA (4:1) micromotors in blood media after micromotor navigation in different drops. IF: Fluorescence intensity